Modelling of Processes in Electro-Hydraulic Valves of an Engine' Fuel System

Oleksandr VRUBLEVSKYI

University of Warmia and Mazury in Olsztyn, Poland, E-mail: aleksander.wroblewski@uwm.edu.pl

Nomenclature

df – damping decrement; E_k – kinetic energy, J; F – force, N; f – cross-section area, m²; h – displacement, m; Q – volume flow rate, m³/s; k – recovery ratio; L – length, m; m – mass, kg; p – fuel pressure, MPa; $q(t)$ – force applied, N; S – cross-section perimeter, m; T – basic oscillation period, s; t – time, s; U – average fuel velocity, m/s; x – distance coordinate, m; z – stiffness coefficient, N/m; μf – effective area, m²; ρ – fuel density, kg/m³; v –kinematic viscosity, m²/s; φ_k – kinetic energy coefficient;

subscripts –
CR – Common Rail fuel system.

1. Introduction

A fuel supply system for heat engines is a good example of high-tech and knowledge-based product. Micron-scale distance and movements, critical dynamic parameters are the signs of that equipment. That means, there are demands to develop and use innovative methods for control, dynamic analysis and hydrodynamic calculations. To improve the performance of electro-hydraulic drive systems, numerous studies are being carried out. The key elements in the modern fuel supply equipment are electro-hydraulic valves with direct or indirect electromagnetic actuators, piezo converters, magnetostriction effect based units. For example, influence of variation of delivery chamber diameter, needle seat semi-angle, needle cone semi-angle, ball valve seat semi-angle, nozzle hole diameter, inlet orifice diameter and outlet orifice diameter on fuel injection quantity had been analyzed [1].

The valves are symbiotic technology of electronic actuators and hydro mechanical design. The fuel supply equipment and its subsystems (unlike the engine in general) are such dynamic objects which could be fully described mathematically, based on direct application of the mechanic laws, as well as electrotechnics and hydraulic laws.

The research results [2-7] show the possibility of improving the characteristics of high-speed electromagnetic drives by optimizing the design [2, 3], the control algorithm [4–6], the use of new magnetic soft materials [7] and smart technologies [8].

There are many works targeted on investigation of processes in the fuel systems with electronic control [9 – 19]. The authors in work [9] investigate the influence of control volume supplying and discharge holes and of their inlet fillet, as well as the effect of the control volume capacity, on the injector performance. In works [10–12] the authors evaluate performance coherence and stability of

injection volume of a diesel engine. This work proposes the way to increase the reliability of the fuel supply mathematical model through description of internal processes from the inside of control units. The computational study has been performed in a multi-hole nozzle at ten different fixed needle lifts, cavitation modelling with a continuous flow in the nozzle model that considers the cavitating nozzle flow as a homogeneous mixture of liquid and vapor, and taking into account the turbulence effects [13–15]. Based on the geometric modelling, assembly the dimension chain of the injector control chamber is established, and the relationship between the assembly tolerance and volume change of the control chamber is analyzed [16]. The simulation result shows that the volume of fuel injection changes correspondingly with a change of the assembly tolerance, while injection rate and pressure do not change significantly and the response rate of the needle is considerably slow. The significant results were obtained in [17, 18], where improvements in the process of controlling of the pressure in the system use models of hydraulic valves with an electromagnetic actuator. Fundamental aspects of the CR fuel injection system dynamics were investigated, paying special attention to the wave propagation induced by pressure oscillations and to its connections with the system control parameters and multiple-injection performance [19]. The analysis of the system oscillation behavior was carried out with the support of a simple lumped parameters model, which makes impossible to study the processes in the hydro mechanical control valve.

The results of those works are being used in designing and creating of the new examples of equipment [11, 20], optimization and modernization of the existing unit designs [21 – 24], also in the new diagnostic approaches [19] and in the specific software [25, 26].

The major number of investigators pay their main attention to processes occurring in volumes with high pressure (250 MPa and higher) [14, 27, 28]. At the same time the processes in the fuel system' control units are being modelled with huge amount of assumptions, but the experimental data show (Fig. 1, 2) that those processes influence on the control valves movements and thus on the fuel injection characteristics.

As it follows from the experimental data (Figs. 1, 2), valve movement h_v in the system filled with fuel and with work pressure level p_c differs from its movement without fuel. The valve stroke damping takes place due to the effect of joint mass; also the maximum valve stroke kinetic energy level changes.

2. Research objective

The main targeted processes to be modelled are

fuel flow processes in the small gaps (up to 0.25 mm), and dynamical parameters in the valve-spring system. The hydro dynamical construction (Fig. 3) is a common wide-spread valve design being used in the CR systems and it is possible to separate four cavities with low pressure A, B, C, D (through those cavities the fuel gets into the drain line):

 − cavity A is between the intake hole of the control chamber and the ring gap between the valve 4 and the injector body;

 − cavity B is between a given gap and the hole in the valve bushing;

 − cavity C is made by the electromagnet anchor 5;

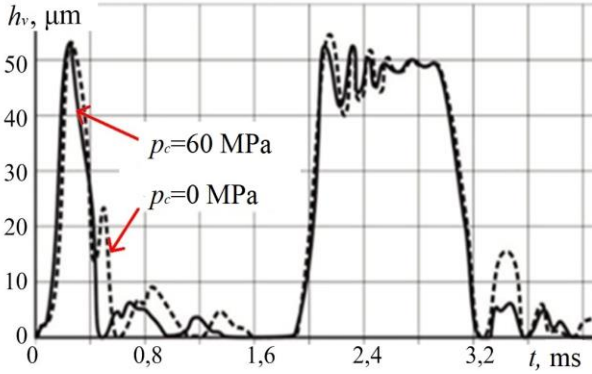 − cavity D is placed above the anchor 5.

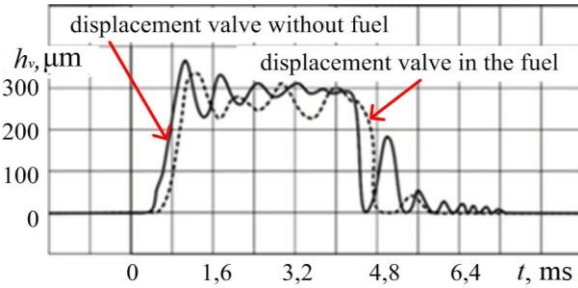Fig. 1 Experimental data for electromagnetic injector valve movements

Fig. 2 Movements of electromagnetic valve in the high-pressure fuel pump
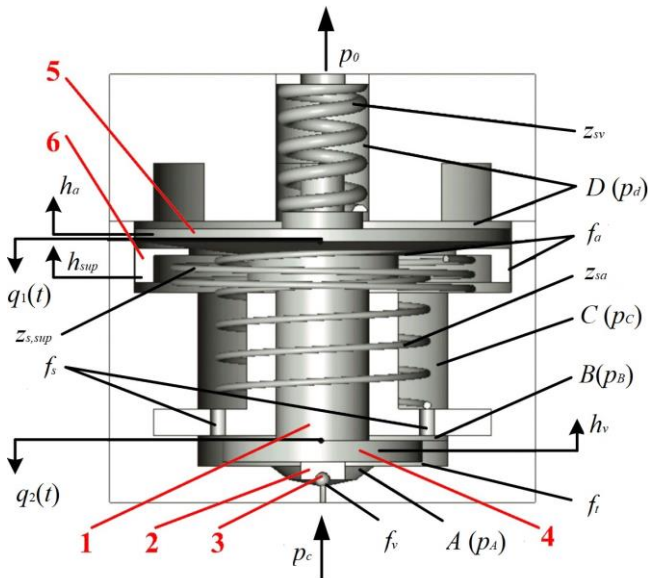

Fig. 3 The scheme of the COMMON RAIL injector control part [29]: *1* – valve; *2* – valve seat; *3* – sphere; *4* – valve part; *5* – anchor; *6* –damper-support

3. Research results

The cylindrical part of the valve *1* (Fig. 3) could be represented as a deformable rod with distributed parameters. The rod at the ends will have a concentrated mass of the obturator valve part (valve seat *2*, sphere *3*, valve part *4*) and the anchor *5*. In this case, the valve and anchor movement equation could be written in the following form:

$$m_v \frac{d^2 h_v}{dt^2} = f_{v2} \cdot p_C + f_{v1} \cdot p_A + f_{v3} \cdot p_{A`} - f_{v4} \cdot p_{B`} - q_2^v(t), \quad (1)$$

where: m_v is a total mass of the locking ball, its seat and the lower valve plate; h_v is the valve displacement; f_{v1}, f_{v2}, f_{v3}, f_{v4} are cross-sections areas of: the ball through the locking belt, ball seat, valve plate ring areas from the side of the cavities B and C; p_A is the fuel pressure in the cavity A; p_B is fuel pressure at the valve seat; $q_2^v(t)$ is the force applied on the ball from the valve stem side,

$$q_2^v(t) = z_c^v \left(\begin{array}{l} h_{0v} + 0{,}5 \Delta h_a(t) + \sum_{j=1}^{t/T_{cv}} df^j \cdot \Delta h_a(t - jT_{cv}) - \\ -0{,}5(1+df) \cdot \sum_{j=0}^{t/T_{cv}-0,5} df^j \cdot \Delta h_v(t - (j+0{,}5) \cdot T_{cv}) \end{array} \right),$$

where: h_{0v} is the pre-deformation of the valve stem; $\Delta h_a(t)$, $\Delta h_v(t)$ are conventional strain from the equation:

$$\Delta h_a = \left(T_{cv} \cdot \dot{h}_a(t) + \frac{2(1-df)}{1+df} \cdot h_a(t) \right),$$

$$\Delta h_v = \left(T_{cv} \cdot \dot{h}_v(t) + \frac{2(1-df)}{1+df} \cdot h_v(t) \right),$$

z_c^v is the valve stem stiffness coefficient; T_{cv} is the valve stem basic oscillation period $T_{cv} = 2\sqrt{m_{cv}/z_{cv}}$; $h_{1v}(t)$ is the valve face displacement from the anchor side, $h_{2v}(t)$– the valve stem face displacement from the ball side; $m_{c\,v}$ is the electromagnetic valve stem mass.

The equation describing anchor movement will be:

$$m_a \frac{d^2 h_a}{dt^2} = f_a \cdot (p_C - p_D) + F - q_1^v(t) + F_{sa}(t) - F_{sv}(t), \quad (2)$$

where: m_a is the mass of the anchor and parts moving with it; h_a is the anchor displacement; $q_1^v(t)$ is the bearing response applied to the anchor from the valve stem side; it could be evaluated from the following:

$$q_1^v(t) = z_c^v \left(\begin{array}{l} h_{0v} + 0{,}5 \Delta h_1^v(t) + \sum_{j=1}^{t/T_s} df^j \cdot \Delta h_1^v(t - jT_c^v) - \\ -0{,}5(1+df) \cdot \sum_{j=0}^{t/T_s-0,5} df^j \cdot \Delta h_2^v(t - (j+0{,}5) \cdot T_c^v) \end{array} \right),$$

where: F is the force applied by the actuator; p_C is the fuel pressure in the cavity C; p_D– fuel pressure in the cavity D; f_a is anchor area from the cavity C side; $F_{sv}(t)$ and $F_{sa}(t)$ are

the valve and anchor spring forces:

$$F_{cv}(t) = z_{cv} \cdot \left(h_{0v} + 0.5\Delta h_a + \sum_{j=1}^{t/T_{cv}} df^{\,j} \cdot \Delta h_a(t - jT_{sv}) \right),$$

$$F_{sa}(t) = z_{sa} \cdot \left(h_{0a} + 0.5\Delta h_a + \sum_{j=1}^{t/T_{cv}} df^{\,j} \cdot \Delta h_a(t - jT_{sa}) \right),$$

h_{0v} is the valve spring pre-deformation; h_{0a}– the anchor spring pre-deformation; z_{sv} is the valve spring stiffness coefficient; z_{sa} is the anchor spring stiffness coefficient; T_{sv}, T_{sa} are the basic oscillation periods for the valve and anchor springs.

The equation describing anchor damper-support movement is:

$$m_{sup} \frac{d^2 h_{sup}}{dt^2} = f_{sup}(p_C - p_D) + F_{s\,sup}(t), \qquad (3)$$

where: m_{sup} is the support mass; h_{sup} is the anchor support displacement; f_{sup} is the support area from the cavity **C** side; $F_{s.sup}(t)$ is the support spring force, being evaluated from:

$$F_{s.sup}(t) = z_{s.sup} \cdot \left(\begin{array}{l} h_{0\,sup} + 0.5\,\Delta h_{sup}(t) + \\ + \sum_{j=1}^{t/T_{s.sup}} df^{\,j} \cdot \Delta h_{sup}(t - jT_{s.sup}) \end{array} \right),$$

$z_{s.sup}$ is the support spring stiffness coefficient; $T_{s.sup}$ is the spring basic oscillation period $T_{s.sup} = 2\sqrt{m_{s.sup}/z_{s.sup}}$; $m_{s.sup}$ is the spring mass.

The time of the anchor and its support joint movement is described by the following equation:

$$(m_a + m_{sup}) \cdot \frac{d^2 h_a}{dt^2} = f'_a \cdot p_C - f''_a \cdot p_D + f_{sup} \cdot (p_C - p_D) +$$

$$+ F - q_1^v(t) + F_{sa}(t) - F_{sv}(t) + F_{s.sup}(t). \qquad (4)$$

As soon as a fuel pressure level inside of those cavities is not higher than 1 MPa and pressure change during the injection time equals only to 0.01 MPa, the fuel compression could be calculated from the fuel flow mathematical description.

The following equations are prepared taking into account the flow continuity. For example, in the cavity A:

$$\mu f_{ball}\sqrt{2/\rho(p_c - p_{A`})} - f_v \dot{h}_v = \mu f_t \sqrt{2/\rho(p_A - p_B)}, \quad (5)$$

where: f_v is the area in the ball locking belt cross-section; is valve movement speed; μf_{ball} is the effective area of the ring cross-section through the control valve sphere; f_t is the valve plate area; p_A is the fuel pressure in the cavity A.

4. Mathematical model refining

Reliability of hydrodynamic processes modelling inside of the control valve could be increased by interven-

tion in the following:
- parts collision during their movements;
- fuel flow in the gaps between supports and moving parts;
- joint mass effects.

4.1. Process of parts collision

There are elements placed inside of the control unit, which can participate in collision processes while moving. The collisions appear when: the lower valve plate reaches its stop, the ball reaches the valve seat, the anchor and anchor support are at their maximum displacement. In actual process during the collision part of the energy is being spent for deformation and internal friction overcoming. The part of the work used for parts deformation gets transformed to the kinetic energy again. This energy is characterized by the recovery ratio k, which is in some degree the body elasticity measure and could be found as: $k = |\dot{h}_g / \dot{h}|$, where $\dot{h}_g$ is body velocity after the collision, $\dot{h}$ is body velocity before the collision. Obviously, the recovery ratio is not only kind of a material parameter, but it also depends on the velocity $\dot{h}$. The conclusion is based on the experimental data for steel, where $k = 5/9$ [29].

In the mathematical model, the rebound process could be taken into account as follows. In end of each calculation time interval Δt, the moving part velocity is determined as:

$$\dot{h}_k = \frac{\dot{h} + F_{\Delta t} \cdot \Delta t}{m + 0.25 \cdot z \cdot T \cdot \Delta t}, \qquad (6)$$

where: $F_{\Delta t}$ is force applied to the body during period Δt; z is the stiffness coefficient; T is the basic oscillation period for the valve spring or the valve support; m is moving mass; $\dot{h}$ is the body velocity in the interval beginning.

The displacement in the end of the interval Δt could be evaluated from the equation (7):

$$h_k = h + \frac{\dot{h} + \dot{h}_k}{2} \cdot \Delta t, \qquad (7)$$

where: h is the displacement in the beginning.

The application of the next algorithm for a part movement and its fixed support collision can be determined according to the scheme in the Fig. 4.
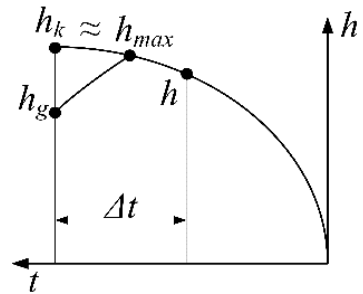

Fig. 4. Scheme of moving part rebound calculation

In the calculation, due to a small step Δt, which equals 0.0007 ms, $h_k = h_{max}$ and evaluating the speed and

the displacement h_g for the moving part after the collision is: $h_g = -k \cdot h_k, h_g = -k \cdot \dot{h}_k$.

It should be mentioned that in this research for the hydro mechanical system it is required to determine the recovery ratio k taking into account real collision process, with fuel in the system. By the calculations of the experimental data, the next k values have been obtained: the multiplier equals $k = 4/9$; the anchor equals $k = 3/9$.

4.2. Fuel flow modelling in the gaps between supports and moving elements

The lower valve plate and the electric magnet anchor during their movements are affected by the additional force, which appears from fuel pressure field between the gaps of the valve plate, the support-limiter of the maximum valve displacement (Fig. 5), the anchor and magnetic core surfaces (Fig. 6). The fuel flow in the mentioned gaps, flow direction and its intensity depend on pressure drops, the mentioned parts velocity direction and the velocity value.
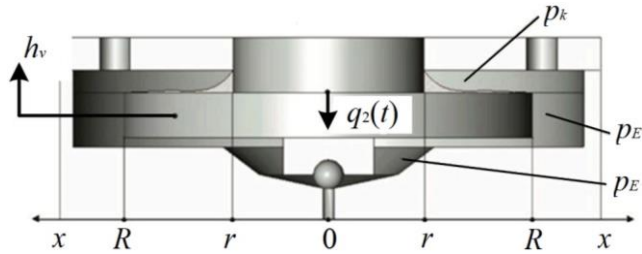

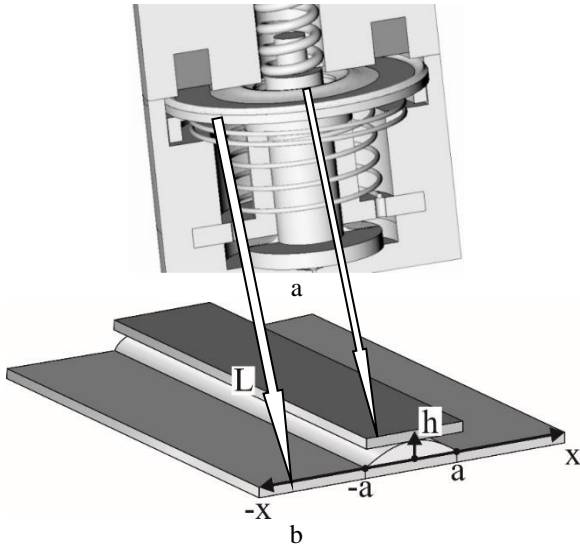Fig. 5 Scheme of the forces applied to the valve

Fig. 6 Fuel flow scheme for the gap between the anchor and the magnetic core: a) 3D model; b) model for calculations

The base of the investigation is the equations of the potential movement of a viscous incompressible fluid in the gaps of 0 – 0.250 mm size. The equations describing this process have the following form.

The fuel velocity and the pressure changes in the gap are described by the next key equations:
- energy balance equation:

$$\frac{d}{dx}\left[\left(p + \phi_k\left(\frac{\rho}{2}\right)U^2\right)Q\right] = -pCS' - \frac{16\nu\rho U^2 S'}{h}, \quad (8)$$

- volume balance equation:

$$\frac{d}{dx}Q = S' \cdot C, \quad (9)$$

where:

$$Q = U \cdot h \cdot S', \quad (10)$$

$U(x)$, $Q(x)$ are average and volumetric fuel speed in the x cross-section, $x \in [r, R]$; S' is a cross-section perimeter, $S' = 2\pi x$; φ_k is the kinetic energy coefficient ($\varphi_k = 4/3$).

The kinetic energy coefficient determines form of the pressure spreading diagram through the given cross-section.

The Eqs. (8) and (9) are generic forms of the well-known Bernoulli's law [31] for the case of the real flow cross-sections (which are proportional to the distance h between a valve and a valve seat) are being changed through time. The right part of the Eq. (8) describes the partial transfer of the mechanical energy from the flow through a given cross-section to the moving valve plate and energy level reduced due to the friction; the left side describes the energy flow changes caused by the losses mentioned above. The Eq. (9) describes changes in velocity of fuel, caused by the real flow changes through cross-section while the valve plate is moving. The Eq. (10) connects the average and volumetric flow velocity values to the $S' \cdot h$ area of its real cross-section. If the flow detaches from the valve - the equation (8) changes to $P(x)=0$ for those cross-sections.

Following the equation (11) integration, it is obtained:

$$Q(x) = \left[S(x) - S(x_0)\right] \cdot C, \quad (11)$$

where: x_0 is the cross-section for zero flow velocity (it corresponds to the radius r); $S(x)$ - the partial area of the valve plate, $S(x) = \pi x^2$.

Using the formulas (10) and (11) in the equation (8) we receive the following:

$$\left(\frac{2}{\rho}\right)\frac{dp}{dx} = -\left[\phi \cdot \left(2 + \frac{x_0^2}{x^2}\right) \cdot C + 32\frac{\nu}{h}\right] \cdot \left(\frac{C}{h^2}\right) \cdot \frac{\left(x^2 - x_0^2\right)}{2x}. \quad (12)$$

In case of the known pressure values p_A and p_B the Eq. (12) allows to determine the pressure field in the gap between the valve and the valve seat, and the value of resultant force F_1 for the fuel pressure applied on the valve. To achieve this, it is needed to integrate the equation for the x coordinate in the area $[r, R]$. After that a biquadratic equation is received to determine the cross-section x_0:

$$\frac{2}{\rho}\left(p_A - p_B\right) =$$

$$= 0,5\left[\left(R^2 - r^2\right)\left(1 - \frac{x_0^4}{\left(R^2 - r^2\right)^2}\right) - x_0^2 ln\left(\frac{R}{r}\right)\right] \times$$

$$\times \varphi\frac{C^2}{h^2} + 8\left[R^2 - r^2 - 2x_0^2 ln\left(\frac{R}{r}\right)\right]v\frac{C}{h^3}. \qquad (13)$$

Solving of the equation lets derive the force F_1 for the case, when $x_0 = r$:

$$F_1 = \pi r^2 p_A + \int_r^R P(x) 2\pi x dx - \pi r^2 p_B.$$

$$F_1 = \pi\frac{\rho}{2}\left(\begin{array}{c}\frac{1}{4}\left(R^2 - r^2\right)\cdot R^2 - r^4 ln\left(\frac{R}{r}\right)\times \\ \times\varphi_k\frac{C^2}{h^2} + 8\left(\left(R^2 - r^2\right)\cdot R^2\right)v\frac{C}{h^3}\end{array}\right). \qquad (14)$$

With the characteristic lifts of the h_v valve, the first terms in formulas (13) and (14) are much larger than the second ones (inertia forces exceed viscosity forces). That is why the solution becomes simpler and the original formula is obtained:

$$F_1 = \pi\frac{\rho}{2}\left\{\left[\frac{1}{4}\left(R^2 - r^2\right)\cdot R^2 - r^4 ln\left(\frac{R}{r}\right)\right]\varphi_k\frac{C^2}{h^2}\right\}. \qquad (15)$$

4.3. Effect of joint mass

In the cavities with low pressure fuel inertia during valve, anchor and its support movements is making the joint mass effect, with value comparable to the masses of the elements. In the modelling of fuel flow through the gap between the anchor and the magnetic core (Fig. 6, a) it can be assumed that the gap is created between the plane and the plate right above it (Fig. 6, b) with width and length adequately $2a$ and L – the perimeter for the average circle clearance.

Considering fuel flow in the narrow gap, the anchor movement velocity could be shown as:

$$\dot{h}(x) = \dot{h}(x/h), \qquad (16)$$

where: x is a coordinate which gives displacement along the clearance cross section, h is the clearance height.

Fuel flow in the clearance is described by the Bernoulli's equation:

$$p(x) + \rho/2\cdot\dot{h}(x) = \rho/2\cdot\dot{h}(a), \qquad (17)$$

or after transformation:

$$p(x) = \rho/2\cdot\dot{h}_0/h^2\cdot\left(a^2 - x^2\right), \qquad (18)$$

where: h_0 is the clearance initial size.

In this case, the force F_1 is:

$$F_1 = 2\cdot L\int_0^a P(x) dx,$$

$$F_1 = 1/3\cdot\rho\cdot\dot{h}_0 S\cdot(a/h)^2, \qquad (19)$$

where: S is the annular area of circular surface of the poles.

The kinetic energy for the fuel in the clearance could be written as:

$$E_k = 0,5\int_0^a m\cdot\dot{h}(x) dx = 0,5\int_0^a \rho\cdot L\cdot\dot{h}(x) dx. \qquad (20)$$

After integrating this equation for coordinate x in the area $[0, a]$ the following equation is obtained:

$$E_k = 1/6 m_{gap}\cdot a^2/h^2\cdot\dot{h}_0, \qquad (21)$$

where: m_{gap} is the fuel mass in the clearance.

Taking into account the total kinetic energy of the anchor and the fuel during movements it is possible to determine the reduced anchor weight:

$$m_{a1} = m_a + 1/3 m_{gap}\cdot a^2/h^2. \qquad (22)$$

The joint mass effect in the cavities with low pressure also appears according to the fuel flow in the channels with a small $(1 - 5\ mm^2)$ cross section (Fig. 7).
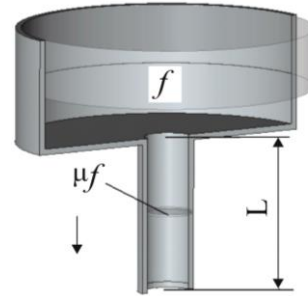

Fig. 7 Fuel flow model in the small cross section channels

The kinetic energy from the fuel, which flows around the damper-anchor support (with flow in the small cross section channels), could be written as:

$$E_k = 0,5\cdot\rho\cdot L\cdot\mu f\cdot\left(f/\mu f\right)^2\cdot\dot{h}_0^2. \qquad (23)$$

So, the reduced mass for the damper-anchor would be:

$$m_{sup1} = m_{sup} + m_t\left(f/\mu f\right)^2, \qquad (24)$$

where: m_t is the fuel mass in the channel of the length L.

In the Eqs. (22, 24) a special attention should be paid to dimensionless multipliers a^2/h^2 and $(f/\mu f)^2$. They allow to determine the dependency between the joint mass effect and the shape of the injector elements – the clearance width to the height ratio or channels area ratio (channels, where fuel flows from one cavity to another one).

The analysis will be carried out for the joint mass

effect at the injector elements. For the anchor width and the clearance of 0.05 mm, the fuel mass equals to 1.2 g in the clearance. This value makes up 30% of the anchor mass, which influences the anchor movement, but at the same time it does not make any change in the movement law.

Taking into account all the processes of fuel movement in the small clearances, Eqs. (1), (2), (3) would be re-written as:

- for the valve:

$$m_v \frac{d^2 h_v}{dt^2} = f_{v2} \cdot p_c + f_{v1} \cdot p_A + f_{v3} \cdot p_{A'} - f_{v4} \cdot p_{B`} - q_2^v(t) - F_1^v,$$

where: F_1^v – the force caused by the fuel pressure field in the clearance between valve plate and the valve displacement limiter;

- for the anchor:

$$m_{a1} \frac{d^2 h_a}{dt^2} = f_a \cdot (p_C - p_D) + F - q_1^v(t) + F_{sa}(t) - F_{sv}(t) - F_1^a,$$

where: F_1^a is the force caused by the fuel pressure field in the clearance between the anchor and the magnetic core;

- for the damper – support:

$$m_{sup1} \frac{d^2 h_{sup}}{dt^2} = f_{sup}(p_C - p_D) + F_{s.sup}(t).$$

The practical value of the received results is the open possibility to determine the effectiveness of the potential changes made to the construction and control algorithms for valves of the given type, for example, the usage of the damper-support 6 (Fig. 3). The calculated results (Figs. 8, 9) show that the damper-support decreases dependency of the anchor (Fig. 9) displacement and the control valve (Fig. 8) from the negative influence of the joint mass effect.

Finally, if the other constant values fuel consumption through the valve decrease from 15.958 mm³ to 14.065 mm³. That lowers energetic expenses in the system in general.
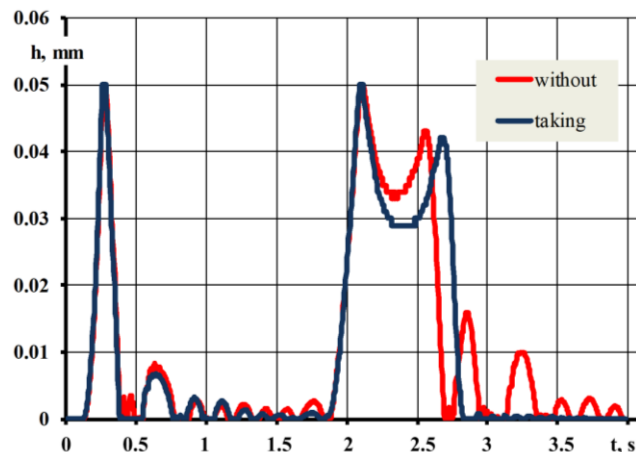

Fig. 8 The result of the simulation of the electro-hydraulic valve stroke without and taking into account the phenomena being investigated
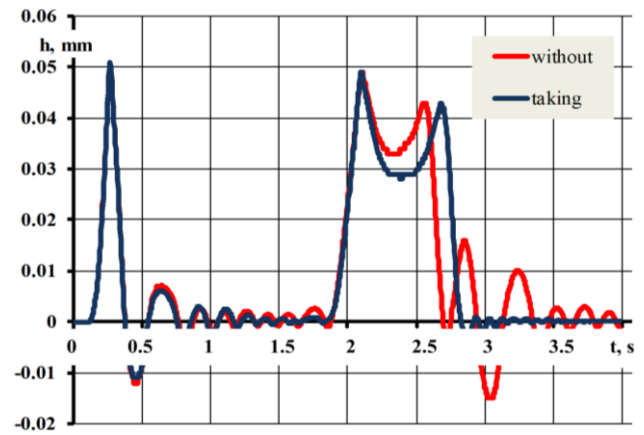

Fig. 9 The result of the modelling of the armature of the electro-hydraulic valve without and taking into account the investigated phenomena

5. Conclusions

The mathematical model describing injector parts movement and fuel flow inside of the control units of the internal combustion engine fuel system is proposed.

Taking into account the moving parts deformation, the movement equations using the models with distributed and lumped parameters for the end masses of the moving parts were elaborated. In addition, the models of the spring allow counting and using oscillations of their coils.

The making the model includes consideration of the following events:
- parts collision during their movement;
- fluid flow in the clearances (smaller than 0.25 mm) between the supports and the moving parts;
- joint masses effect.

The achieved results show that the longitudinal deformations of the valve rod could provide up to 40% of the maximum valve displacement.

The results of the investigation are the propositions for construction and control algorithm improvements for the control units of the given type of the fuel supply system.

References

1. **Bai, Y.; Fan, L.Y.; Ma, X.Z.; Peng, H.L.; Song, E.Z.** 2016. Effect of injector parameters on the injection quantity of common rail injection system for diesel engines, International Journal of Automotive Technology 17(4): 567-579.
https://doi.org/10.1007/s12239-016-0057-2.

2. **Liu, P.; Fan, L.; Hayat, Q.; Xu, D.; Ma, X.; Song, E.** 2014. Research on key factors and their interaction effects of electromagnetic force of high-speed solenoid valve, Scientific World Journal 2014, Article ID 567242: 1-13.
http://dx.doi.org/10.1155/2014/567242.

3. **Sun, Z.-Y.; Li, G.-X.; Wang, L.; Wang, W.-H.; Gao, Q.-X.; Wang, J.** 2016. Effects of structure parameters on the static electromagnetic characteristics of solenoid valve for an electronic unit pump, Energy Conversion and Management113: 119-130.
https://doi.org/10.1016/j.enconman.2016.01.031.

4. **Chung, S. K.; Koch, C. R.; Lynch, A. F.** 2007. Flat-

ness-based feedback control of an automotive solenoid valve, IEEE Transactions on Control Systems Technology 15(2): 394-401.
http://dx.doi: 10.1109/TCST.2006.886440.

5. **Liu, H.; Gu, H.; Chen, D.** 2008. Application of high-speed solenoid valve to the semi-active control of landing gear, Chinese Journal of Aeronautics 21(3): 232-240.
https://doi.org/10.1016/S1000-9361(08)60030-8.

6. **Zhao, J.; Fan, L.; Liu, P.;Grekhov L.; Ma, X.; Song, E.** 2017. Investigation on electromagnetic models of high-speed solenoid valve for common rail injector, Mathematical Problems in Engineering 2017: 1-10.
https://doi.org/10.1155/2017/9078598.

7. **Wang, Q.; Yang, F.; Yang, Q.; Chen, J.; Guan, H.** 2011. Experimental analysis of new high-speed powerful digital solenoid valves, Energy Conversion and Management 52(5): 2309-2313.
http://dx.doi.org/10.1016/j.enconman.2010.12.032.

8. **Worden, K.; Bullough, W. A.; Haywood, J.** 2003. The smart approach - an introduction to smart technologies. In K. Worden, W. A. Bullough, & J. Haywood (Eds.), Smart technologies. River Edge: World Scientific

9. **Coppo, M.; Dongiovanni, C.; Negri, C.** 2004. Numerical analysis and experimental investigation of a common rail-type diesel injector, Journal of Engineering for Gas Turbines and Power 126(4): 874-885.
http://dx.doi:10.1115/1.1787502.

10. **Bingqi, T.; Liyun, F.; Xiuzhen, M.; Hayat, Q.; Yun, B.; Yang, L.** 2014. Investigation of main injection quantity fluctuation due to pilot injection in high pressure common rail fuel injection system, China International Journal On Smart Sensing and Intelligent Systems 7(2): 820-836.

11. **Wang, H.P.; Zheng, D.; Tian Y.** 2016. High pressure common rail injection system modelling and control, ISA Transactions 63: 265-273.
https://doi: 10.1016/j.isatra.2016.03.002.

12. **Wang, M.; Ouyang, G.; Zhou, J.** 2011. Simulation and experimental study on high pressure common rail fuel system of diesel engine, Proceedings of international conference on computer distributed control and intelligent environmental monitoring: 586-9.

13. **Salvado, F. J.;** et al. 2013. Study of the influence of the needle lift on the internal flow and cavitation phenomenon in diesel injector nozzles by CFD using RANS methods, Energy conversion and management 66: 246-256.
http://dx.doi:10.1016/j.enconman.2012.10.011.

14. **Duan, L.; Yuan, S.; Hu, L.F.; Yang, W.-M.; Yu, J.; Xia X.** 2016. Injection performance and cavitation analysis of an advanced 250 MPa common rail diesel injector, International Journal of Heat and Mass Transfer 93: 388-397.
http://dx.doi.org/10.1016/j.ijheatmasstransfer.2015.10.028.

15. **Sun, Z.-Y.; Li, G.-X.; Chen, C.; Yu, Y.-S.; Gao, G.-X.** 2015. Numerical investigation on effects of nozzle's geometric parameters on the flow and the cavitation characteristics within injector's nozzle for a high-pressure common-rail di diesel engine, Energy Conversion and Management 89: 843-861.
https://DOI: 10.1016/j.enconman.2014.10.047.

16. **Jiping, L.; Shuiyuan, T.; Yong, Z.; Jing, H.; Zhonghua, J.** 2011. Simulation of assembly tolerance and characteristics of high pressure common rail injector, International Journal of Computational Intelligence Systems 4(6): 1282-1289.
https://doi.org/10.1080/18756891.2011.9727877.

17. **Gupta, V.K.; Zhang, Z.; Sun, Z.X.** 2011. Modelling and control of a novel pressure regulation mechanism for common rail fuel injection systems, Applied Mathematical Modelling 35: 3473-3483.
https://doi.org/10.1016/j.apm.2011.01.008.

18. **Hong, S; Shin, H.; Sohn, J.; Park, I.; Sunwoo, M.** 2014. Coordinated control strategy for the common-rail pressure using a metering unit and a pressure control valve in diesel engines, Proceedings of the Institution of Mechanical Engineers, Part D: Journal of Automobile Engineering 229(7): 898-911.
https://doi.org/10.1177/0954407014549062.

19. **Catania, A. E.; Ferrari, A.; Manno, M. Spessa, E.** 2008. Experimental investigation of dynamics effects on multiple-injection common rail system performance, Journal of Engineering for Gas Turbines and Power 130: 1-13.
https://doi: 10.1115/1.2835353.

20. **Bianchi, G.M.; Pelloni, P.; Falfari, S.; Brusiani F.; Parotto, M.; Osbat, G.; Lamberti, C.** 2005.Advanced modelling of a new diesel fast solenoid injector and comparison with experiments, SAE Transactions-SAE Journal of Engines 113(3): 1-14.

21. **Shin, Y.; Lee, S.; Choi, C.; Kim, J.** 2015. Shape optimization to minimize the response time of direct-acting solenoid valve, Journal of Magnetics 20(2): 193-200.
http://dx.doi.org/10.4283/JMAG.2015.20.2.193.

22. **Bianchi, G. M.; Pelloni, P.; Filicori, F.; Vannini, G.** 2000. Optimization of Solenoid valve behavior in common-rail injection systems, SAE paper 2000-01-2042.
https://doi.org/10.4271/2000-01-2042.

23. **Wang, Y.; Megli, T.; Haghgooie, M.; Peterson, K. S.; Stefanopoulou, A. G.** 2002. Modelling and control of electromechanical valve actuator, SAE paper 2002-01-1106.
https://doi.org/10.4271/2002-01-1106.

24. **Huber, B.; Ulbrich, H.** 2014. Modelling and experimental validation of the solenoid valve of a common rail diesel injector, SAE paper2014-01-0195.
https://doi.org/10.4271/2014-01-0195.

25. AVL Boost – Hydsim 2013. User's Guide. Graz. Austria.

26. LMS Simens2013. User's Guides of AMESim Rev12.

27. **Xia, S. H.; Zhen, J. B.; Miao, X. L.;** et al. 2012. Cavitation analysis on ball valve in solenoid injector, Transaction CSICE 30(4): 354–358.

28. **Sun, Z. Y.; Li, G. X.; Yu, Y. S.; Gao, S. C.; Gao, G. X.** 2015. Numerical investigation on transient flow and cavitation characteristic within nozzle during the oil drainage process for a high-pressure common-rail DI diesel engine, Energy Conversion and Management 98: 507–517.
http://dx.doi.org/10.1016/j.enconman.2015.04.001.

29. **Mollenhauer, K.; Tschöke, H.** 2010. Handbook of Diesel Engines. Springer-Verlag. Berlin. Heidelberg.

30. **Kuchling, H.** 2001. Taschenbuch der Physik, Carl Hanser Verlag, München.
31. **Nakayama, Y.** 1998. Introduction to Fluid Mechanics, Butterworth-Heinemann.

O. Vrublevskyi

MODELLING OF PROCESSES INTO
ELECTRO-HYDRAULIC VALVES OF AN ENGINE'
FUEL SYSTEM

S u m m a r y

This work proposes the way to increase reliability of fuel feeding mathematical model by taking into account processes from the inside of electro-hydraulic valves - like parts collision during their movements; fuel flow in the clearances between the supports and moving parts; effect of joint mass. The equations to describe the mentioned processes and modelling results are shown. Practical value for received results is the possibility to evaluate effectiveness for changes proposed to be made in the construction and designed control algorithms for multipurpose valves of the given type.